

Task-Aware Delegation Cues for LLM Agents

XINGRUI GU, University of California, Berkeley, USA

LLM agents increasingly present as conversational collaborators, yet human-agent teamwork remains brittle due to information asymmetry: users lack task-specific reliability cues, and agents rarely surface calibrated uncertainty or rationale. We propose a task-aware collaboration signaling layer that turns offline preference evaluations into online, user-facing primitives for delegation. Using Chatbot Arena pairwise comparisons, we induce an interpretable task taxonomy via semantic clustering, then derive (i) Capability Profiles as task-conditioned win-rate maps and (ii) Coordination-Risk Cues as task-conditioned disagreement (tie-rate) priors. These signals drive a closed-loop delegation protocol that supports common-ground verification, adaptive routing (primary vs. primary+auditor), explicit rationale disclosure, and privacy-preserving accountability logs. Two predictive probes validate that task typing carries actionable structure: cluster features improve winner prediction accuracy and reduce difficulty prediction error under stratified 5-fold cross-validation. Overall, our framework reframes delegation from an opaque system default into a visible, negotiable, and auditable collaborative decision, providing a principled design space for adaptive human-agent collaboration grounded in mutual awareness and shared accountability.

1 Introduction

LLM-based agent systems have quickly moved from “tools” to conversational collaborators capable of dialogue, reasoning, and multi-step planning [6, 21, 23, 27]. Yet collaborator-like behavior does not guarantee effective collaboration [1, 28]. Relative to human teams, human-agent interaction still lacks core collaborative properties—mutual awareness, adaptivity, and shared accountability [11, 13, 18]. Users often cannot assess an agent’s task-specific competence, reliability, or failure modes [18], while agents rarely surface calibrated uncertainty or decision rationale [26]. The resulting opacity makes interactions brittle and failures hard to diagnose or repair [24]. In distributed teamwork, collaborators compensate for limited shared context through explicit signaling to establish common ground and accountability [4, 8]. Analogously, human-agent collaboration is characterized by information asymmetry—users lack actionable reliability cues and agents lack standardized channels to communicate rationale and uncertainty—leading to trust miscalibration and an accountability vacuum when errors occur [1, 17, 22].

A central challenge is deciding which agent is most reliable for a given delegation and when to trigger interventions such as clarification or dual verification [2, 7, 15, 16, 25]. Existing methods often depend on coarse global rankings that miss task-specific brittleness—models may excel in one domain yet hallucinate in another—and rarely adapt to intrinsic task ambiguity [3, 25].

Author’s Contact Information: [Xingrui Gu](#), xingrui_gu@berkeley.edu, University of California, Berkeley, Berkeley, CA, USA.

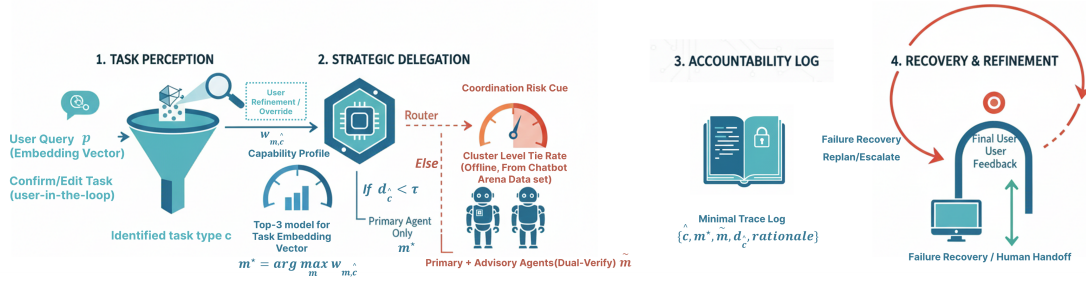


Fig. 1. **The Task-Aware Delegation & Awareness Loop.** Our framework operationalizes (1) Intent Recognition via semantic clustering, (2) Dynamic Delegation based on capability profiles, (3) Awareness Cues for trust calibration, and (4) Accountability Logging for error recovery.

We propose a task-aware collaboration signaling layer that turns offline capability assessments into online, user-facing cues. Combining semantic task clustering with large-scale human preference data, we derive task-conditioned Capability Profiles and Uncertainty Cues, which drive a closed-loop delegation protocol (task typing \rightarrow routing \rightarrow explicit rationale \rightarrow accountable logging). This reframes delegation from an opaque default into a visible, negotiable, and auditable collaborative decision, supporting calibrated trust and adaptive human-agent teamwork [1, 18, 24].

2 Related Work: Agents as Remote Collaborators

A burgeoning perspective in Human-Computer Interaction (HCI) frames intelligent agents not merely as tools, but as *remote collaborators* [1]. This conceptual shift draws on classic CSCW insights into distributed teamwork, where the absence of a shared physical environment necessitates a reliance on explicit signaling to establish **common ground** [4, 19]. As defined by Media Richness Theory, text-based interaction—despite using natural language—often functions as a relatively “lean” channel compared to face-to-face collaboration [5]. In such environments, the agent’s internal reasoning, capability boundaries, and uncertainty are often obscured, leading to systemic information asymmetry and making appropriate reliance difficult [1, 10, 17, 18]. Previous studies have shown that reduced shared context and limited cues can increase grounding/coordination costs in remote collaboration [9, 11, 13, 19], while miscalibrated trust can result in misuse/disuse when failures occur [12, 14, 17, 20]. This theoretical backdrop suggests that for LLM agents to become genuine partners, they must move beyond task execution toward proactive signaling of their task-specific reliability and context.

3 Preference-Derived Collaboration Signals

We derive task-conditioned collaboration signals from human preference comparisons, capturing (i) *capability* (who tends to win on a task type) and (ii) *coordination risk* (when disagreement is high and additional grounding/auditing is warranted).

3.1 Task typing

Given prompts $\mathcal{P} = \{p_i\}_{i=1}^N$, we obtain semantic embeddings

$$e_i = f_{\text{enc}}(p_i) \in \mathbb{R}^d, \quad (1)$$

apply a standard dimensionality reduction operator $g(\cdot)$ (e.g., UMAP), and perform K-means clustering to obtain a task type $c_i \in \{1, \dots, K\}$ for each prompt:

$$x_i = g(e_i), \quad c_i = \text{KMeans}(x_i), \quad K = 30. \quad (2)$$

Equivalently, K-means solves

$$\arg \min_{\{C_j\}_{j=1}^K} \sum_{j=1}^K \sum_{x_i \in C_j} \|x_i - \mu_j\|_2^2, \quad (3)$$

where μ_j is the centroid of cluster C_j . We optionally assign human-readable labels to clusters via representative keywords for presentation. Figure 3 visualizes the induced task-typing structure in a low-dimensional projection.

3.2 Capability profile

Each prompt p_i is associated with a human comparison record (p_i, m_A, m_B, y_i) where $y_i \in \{m_A, m_B, \text{tie}\}$.

For each agent/model m and task cluster c , we define the empirical win rate

$$w_{m,c} = \frac{1}{|\mathcal{D}_{m,c}|} \sum_{(i,y_i) \in \mathcal{D}_{m,c}} \mathbb{I}[y_i = m], \quad (4)$$

where $\mathcal{D}_{m,c}$ denotes comparisons involving m on prompts with $c_i = c$. We treat $w_{m,c}$ as a task-conditioned capability signal. Figure 6 shows that winner distributions differ substantially across task types, supporting task-conditioned capability profiling.

3.3 Coordination risk cue

We quantify task-conditioned uncertainty via the tie rate within each cluster:

$$d_c = \frac{1}{|\mathcal{D}_c|} \sum_{(i,y_i) \in \mathcal{D}_c} \mathbb{I}[y_i = \text{tie}], \quad (5)$$

where \mathcal{D}_c collects all comparisons with $c_i = c$. We interpret d_c as a *coordination-risk cue* (model disagreement / ambiguity), rather than a ground-truth hardness measure. Figure 2 reports the task-type-level uncertainty proxy used as a coordination-risk cue.

4 Experiments: Validating Task-Conditioned Collaboration Signals

Section 3 introduces two task-conditioned signals from preference data: a *capability profile* (task-specific win tendency) and a *coordination-risk cue* (high disagreement/uncertainty). We evaluate their behavioral validity using two probes on Chatbot-Arena-style pairwise comparisons: (A) **winner prediction** and (B) **difficulty prediction**. Task A tests whether task typing explains systematic, task-dependent performance differences; Task B tests whether task type and disagreement jointly predict perceived difficulty, justifying disagreement-based risk cues.

Dataset and evaluation protocol. We use the Chatbot Arena dataset [3], which consists of single-turn prompts paired with human preference comparisons between two LLMs, denoted by (p_i, m_A, m_B, y_i) , where $y_i \in \{m_A, m_B, \text{tie}, \text{invalid}\}$. Each record also includes prompt metadata and embedding features. We report stratified 5-fold cross-validation (CV) performance and compare regularization choices across models.

Task A: Model winner classification. Task A predicts the outcome of a pairwise comparison (A wins / B wins / tie / invalid). We use multinomial logistic regression for interpretability. Feature engineering follows three groups: (i) one-hot model identities for both contestants, (ii) one-hot task cluster c_i from Section 3.1, and (iii) response-embedding difference $e_A - e_B$.

Task B: Prompt difficulty prediction. Task B predicts a prompt difficulty score (1–10). We use Ridge regression and evaluate with MSE. Features include (i) task cluster identity (capturing task-type-level difficulty trends), (ii) winner-combination indicators (capturing disagreement patterns), and (iii) prompt length.

Results. Table 1 shows that Ridge regularization performs best for both tasks under 5-fold CV, which also isolates the contribution of task typing: removing cluster features reduces Task A accuracy and increases Task B MSE, supporting the predictive value of task-conditioned signals for both capability and coordination risk.

5 Delegation Protocol

We operationalize the task-conditional capability profiles $w_{m,c}$ (Eq. 4) and collaborative risk cues d_c (Eq. 5) into an online delegation process, formalized in Algorithm 1. Here, the cluster-level tie-rate d_c , defined in Section 3.3, serves as a proxy for uncertainty and disagreement to characterize task-conditional coordination risks. Given a user request p , the system first predicts the task category

Algorithm 1 Task-aware Delegation with Capability & Coordination-Risk Cues

Require: user request p ; task typer $\hat{c} = \text{Type}(p)$; capability $w_{m,c}$ (Eq. 4); risk cue d_c (tie-rate, Eq. 5); threshold τ

- 1: **Type & verify:** show \hat{c} (with rationale/confidence); allow user override $\hat{c} \leftarrow \text{Edit}(\hat{c})$
- 2: **Delegate:** $m^* \leftarrow \arg \max_m w_{m,\hat{c}}$ ▷ primary collaborator
- 3: **if** $d_{\hat{c}} > \tau$ **then**
- 4: $\tilde{m} \leftarrow \arg \max_{m \neq m^*} w_{m,\hat{c}}$ ▷ auditor / backup
- 5: trigger safeguard(s): {one clarification, auditing, cite sources, stepwise plan}
- 6: **else**
- 7: $\tilde{m} \leftarrow \emptyset$
- 8: **end if**
- 9: **Expose awareness cues:** report delegation rationale using $(w_{m,\hat{c}}, d_{\hat{c}})$ and active strategy
- 10: **Accountability log:** record $\{\hat{c}, m^*, \tilde{m}, d_{\hat{c}}, \text{safeguards, repair/handoff}\}$ under privacy constraints
- 11: **Execute:** generate output with m^* ; optionally audit with \tilde{m}

\hat{c} , allowing for user overrides to establish *common ground*. Subsequently, the system selects the primary collaborator $m^*(\hat{c}) = \arg \max_m w_{m,\hat{c}}$. If the risk signal exceeds a threshold ($d_{\hat{c}} > \tau$), a high-assurance mode is triggered (e.g., seeking clarification, auditing, or grounding), potentially assigning an auxiliary auditor $\tilde{m}(\hat{c})$. Before execution, the system explicitly surfaces delegation rationales based on $(w_{m,\hat{c}}, d_{\hat{c}})$ and maintains a minimized, privacy-preserving *accountability log* to support error recovery and retrospective auditing. In high-disagreement scenarios ($d_{\hat{c}} > \tau$), the system proactively poses a clarifying question and enables cross-verification by \tilde{m} . Conversely, in low-disagreement tasks ($d_{\hat{c}} \leq \tau$), the system prioritizes efficiency by executing the task directly through m^* to minimize coordination overhead.

5.1 Risks and Safeguards.

(1) **Bias Amplification:** Semantic clustering may **reify** representational biases. To counteract this, our protocol mandates user-editable task labels and provides interpretable classification rationales to support human-in-the-loop auditing. (2) **Trust Miscalibration:** High performance scores ($w_{m,c}$) can induce user over-reliance. We mitigate this by mandating the disclosure of model limitations and surfacing risk-adjusted strategies whenever $d_{\hat{c}} > \tau$, fostering a more critical and calibrated trust. (3) **Privacy Inference:** Aggregated task logs could potentially facilitate sensitive user profiling. The protocol enforces **minimalist data retention** by default, provides granular “right-to-be-forgotten” mechanisms, and applies noise to logging frequency in high-sensitivity task clusters.

References

- [1] Saleema Amershi, Dan Weld, Mihaela Vorvoreanu, Adam Fourney, Besmira Nushi, Penny Collisson, Jina Suh, Shamsi Iqbal, Paul N Bennett, Kori Inkpen, et al. 2019. Guidelines for human-AI interaction. In *Proceedings of the 2019 chi conference on human factors in computing systems*. 1–13.
- [2] Lingjiao Chen, Matei Zaharia, and James Zou. 2023. Frugalgpt: How to use large language models while reducing cost and improving performance. *arXiv preprint arXiv:2305.05176* (2023).
- [3] Wei-Lin Chiang, Lianmin Zheng, Ying Sheng, Anastasios Nikolas Angelopoulos, Tianle Li, Dacheng Li, Banghua Zhu, Hao Zhang, Michael Jordan, Joseph E Gonzalez, et al. 2024. Chatbot arena: An open platform for evaluating llms by human preference. In *Forty-first International Conference on Machine Learning*.
- [4] Herbert H Clark and Susan E Brennan. 1991. Grounding in communication. (1991).
- [5] Richard L Daft and Robert H Lengel. 1986. Organizational information requirements, media richness and structural design. *Management science* 32, 5 (1986), 554–571.
- [6] Paramveer S Dhillon, Somayeh Molaei, Jiaqi Li, Maximilian Golub, Shaochun Zheng, and Lionel Peter Robert. 2024. Shaping human-AI collaboration: Varied scaffolding levels in co-writing with language models. In *Proceedings of the 2024 CHI Conference on Human Factors in Computing Systems*. 1–18.
- [7] Shehzaad Dhuliawala, Mojtaba Komeili, Jing Xu, Roberta Raileanu, Xian Li, Asli Celikyilmaz, and Jason Weston. 2024. Chain-of-verification reduces hallucination in large language models. In *Findings of the association for computational linguistics: ACL 2024*. 3563–3578.
- [8] Melanie Duckert, Louise Barkhuus, and Pernille Bjørn. 2023. Collocated distance: a fundamental challenge for the design of hybrid work technologies. In *Proceedings of the 2023 CHI conference on human factors in computing systems*. 1–16.
- [9] Susan R Fussell, Robert E Kraut, and Jane Siegel. 2000. Coordination of communication: Effects of shared visual context on collaborative work. In *Proceedings of the 2000 ACM conference on Computer supported cooperative work*. 21–30.
- [10] Xingrui Gu and Chuyi Jiang. [n. d.]. Laplacian Flows for Policy Learning from Experience. In *ICLR 2026 Workshop on Geometry-grounded Representation Learning and Generative Modeling*.
- [11] Xingrui Gu, Chuyi Jiang, Erte Wang, Zekun Wu, Qiang Cui, Leimin Tian, Lianlong Wu, Siyang Song, and Chuang Yu. 2025. CauSkelNet: Causal Representation Learning for Human Behaviour Analysis. In *2025 IEEE 19th International Conference on Automatic Face and Gesture Recognition (FG)*. IEEE, 1–13.
- [12] Xingrui Gu, Guanren Qiao, Chuyi Jiang, TianQing Xia, and Hangyu Mao. 2024. Mimicking Human Intuition: Cognitive Belief-Driven Q-Learning. (2024).
- [13] Xingrui Gu, Zhixuan Wang, Irisa Jin, and Zekun Wu. 2024. Advancing Pain Recognition Through Statistical Correlation-Driven Multimodal Fusion. In *2024 12th International Conference on Affective Computing and Intelligent Interaction Workshops and Demos (ACIIW)*. IEEE, 281–289.
- [14] Xingrui Gu and Haixi Zhang. [n. d.]. Uncertainty-Gated Generative Modeling. In *The 2nd Workshop on Advances in Financial AI Workshop: Towards Agentic and Responsible Systems*.
- [15] Eric Horvitz. 1999. Principles of mixed-initiative user interfaces. In *Proceedings of the SIGCHI conference on Human Factors in Computing Systems*. 159–166.
- [16] Zhongzhan Huang, Guoming Ling, Yupei Lin, Yandong Chen, Shanshan Zhong, Hefeng Wu, and Liang Lin. 2025. Routereval: A comprehensive benchmark for routing llms to explore model-level scaling up in llms. *arXiv preprint arXiv:2503.10657* (2025).

- [17] John D Lee and Katrina A See. 2004. Trust in automation: Designing for appropriate reliance. *Human factors* 46, 1 (2004), 50–80.
- [18] Margaret Mitchell, Simone Wu, Andrew Zaldivar, Parker Barnes, Lucy Vasserman, Ben Hutchinson, Elena Spitzer, Inioluwa Deborah Raji, and Timnit Gebru. 2019. Model cards for model reporting. In *Proceedings of the conference on fairness, accountability, and transparency*. 220–229.
- [19] Gary M Olson and Judith S Olson. 2000. Distance matters. *Human–computer interaction* 15, 2-3 (2000), 139–178.
- [20] Raja Parasuraman and Victor Riley. 1997. Humans and automation: Use, misuse, disuse, abuse. *Human factors* 39, 2 (1997), 230–253.
- [21] Joon Sung Park, Joseph O’Brien, Carrie Jun Cai, Meredith Ringel Morris, Percy Liang, and Michael S Bernstein. 2023. Generative agents: Interactive simulacra of human behavior. In *Proceedings of the 36th annual acm symposium on user interface software and technology*. 1–22.
- [22] Filippo Santoni de Sio and Jeroen Van den Hoven. 2018. Meaningful human control over autonomous systems: A philosophical account. *Frontiers in Robotics and AI* 5 (2018), 323836.
- [23] Timo Schick, Jane Dwivedi-Yu, Roberto Dessì, Roberta Raileanu, Maria Lomeli, Eric Hambro, Luke Zettlemoyer, Nicola Cancedda, and Thomas Scialom. 2023. Toolformer: Language models can teach themselves to use tools. *Advances in Neural Information Processing Systems* 36 (2023), 68539–68551.
- [24] Hetan Shah. 2018. Algorithmic accountability. *Philosophical Transactions of the Royal Society A: Mathematical, Physical and Engineering Sciences* 376, 2128 (2018), 20170362.
- [25] Alberto Testoni and Raquel Fernández. 2024. Asking the right question at the right time: Human and model uncertainty guidance to ask clarification questions. *arXiv preprint arXiv:2402.06509* (2024).
- [26] Zhengtao Xu, Tianqi Song, and Yi-Chieh Lee. 2025. Confronting verbalized uncertainty: Understanding how LLM’s verbalized uncertainty influences users in AI-assisted decision-making. *International Journal of Human-Computer Studies* 197 (2025), 103455.
- [27] Shunyu Yao, Jeffrey Zhao, Dian Yu, Nan Du, Izhak Shafran, Karthik R Narasimhan, and Yuan Cao. 2022. Re-act: Synergizing reasoning and acting in language models. In *The eleventh international conference on learning representations*.
- [28] Rui Zhang, Nathan J McNeese, Guo Freeman, and Geoff Musick. 2021. " An ideal human" expectations of AI teammates in human-AI teaming. *Proceedings of the ACM on Human-Computer Interaction* 4, CSCW3 (2021), 1–25.

A Implementation Details: Task Typing and Preference Modeling

This appendix details the end-to-end implementation of task typing (semantic clustering), preference alignment, and the two predictive probes (Task A/B) used in Sec. 4. Our goal is reproducibility: we specify inputs, preprocessing, hyperparameters, and evaluation.

A.1 Inputs and data representation

We assume a dataset of prompts and pairwise preference comparisons:

$$\mathcal{P} = \{p_i\}_{i=1}^N, \quad \mathcal{D} = \{(p_i, m_A, m_B, y_i)\},$$

where $y_i \in \{m_A, m_B, \text{tie}, \text{invalid}\}$. Each prompt is assigned a task type $c_i \in \{1, \dots, K\}$ via semantic clustering (Sec. A.2), and comparisons are aligned to clusters for computing task-conditioned statistics (Sec. A.3).

A.2 Semantic embedding and task clustering

Prompt embeddings. We embed each prompt using a pretrained sentence encoder f_{enc} (Sentence-BERT):

$$e_i = f_{\text{enc}}(p_i) \in \mathbb{R}^d. \quad (6)$$

Dimensionality reduction. To improve clusterability and reduce noise, we apply a standard manifold learning operator $g(\cdot)$ (e.g., UMAP) to obtain $x_i = g(e_i) \in \mathbb{R}^{d'}$ with $d' \ll d$. For completeness, UMAP optimizes a cross-entropy objective that preserves neighborhood structure; we refer to the UMAP paper for the full derivation.

Clustering. We run K -means on $\{x_i\}$ with $K = 30$ to obtain clusters $\{C_j\}_{j=1}^K$:

$$\arg \min_{\{C_j\}_{j=1}^K} \sum_{j=1}^K \sum_{x_i \in C_j} \|x_i - \mu_j\|_2^2, \quad (7)$$

where μ_j is the centroid of cluster C_j . To reduce fragmentation, clusters with size below a threshold δ are reassigned to the nearest large cluster by centroid distance:

$$C_{\text{target}} = \arg \min_{j \in \mathcal{L}} \|\mu_{\text{small}} - \mu_j\|_2, \quad (8)$$

where \mathcal{L} indexes clusters with size $\geq \delta$.

Cluster presentation. For interpretability in the UI/protocol layer, we optionally attach a short label to each cluster via representative keywords (e.g., top-frequency tokens after standard text preprocessing).

A.3 Preference alignment and signal computation

Each comparison $(p_i, m_A, m_B, y_i) \in \mathcal{D}$ is aligned to the cluster of its prompt c_i . We compute two task-conditioned signals used in Sec. 3:

Capability profile (win-rate). For each model m and cluster c , we compute

$$w_{m,c} = \frac{1}{|\mathcal{D}_{m,c}|} \sum_{(i,y_i) \in \mathcal{D}_{m,c}} \mathbb{I}[y_i = m], \quad (9)$$

where $\mathcal{D}_{m,c}$ denotes comparisons involving m whose prompt has $c_i = c$.

Coordination-risk cue (tie-rate). We quantify task-conditioned uncertainty/disagreement via the cluster tie-rate:

$$d_c = \frac{1}{|\mathcal{D}_c|} \sum_{(i,y_i) \in \mathcal{D}_c} \mathbb{I}[y_i = \text{tie}], \quad (10)$$

where \mathcal{D}_c contains all comparisons with $c_i = c$. In the main paper, d_c is treated as a coordination-risk proxy rather than a ground-truth hardness label.

A.4 Pipeline pseudocode

A.5 Experiment details: predictive probes (Task A/B)

We include two predictive probes to validate that task typing carries signal beyond global model identity.

Task A: winner prediction (classification). Task A is a 4-class classification problem predicting $y_i \in \{\text{A wins, B wins, tie, invalid}\}$. We use multinomial logistic regression for interpretability. *Invalid* comparisons can be either (i) retained as a separate class or (ii) excluded from training; we follow the main-text setting and report results accordingly.

Features. We concatenate three feature groups: (i) model identity one-hots for the two contestants (40 binary features for 20 LLMs); (ii) task cluster one-hot (30 binary features); and (iii) response-embedding difference $e_{\text{diff}} = e_A - e_B$ (256 numeric features), yielding a 326-dimensional vector.

Task B: difficulty prediction (regression). Task B predicts a scalar prompt difficulty score (1–10). We use Ridge regression and evaluate by MSE. *Features.* We use (i) task cluster one-hot (30), (ii) winner-combination indicators (5), and (iii) prompt length (1), for a 36-dimensional vector.

Evaluation protocol. We report stratified 5-fold cross-validation. We compare regularization choices (None / Ridge / Lasso) and include an ablation that removes the cluster one-hot features to quantify the contribution of task typing.

Algorithm 2 End-to-end Pipeline: Task Typing \rightarrow Preference Signals \rightarrow Validation Probes

Require: Prompts $\mathcal{P} = \{p_i\}_{i=1}^N$; pairwise comparisons $\mathcal{R} = \{(p_i, m_A, m_B, y_i)\}$ with $y_i \in \{m_A, m_B, \text{tie}, \text{invalid}\}$; encoder f_{enc} ; reducer g (e.g., UMAP); K clusters; CV folds F

Ensure: Task labels $\{c_i\}$; capability profiles $\{w_{m,c}\}$; coordination-risk cues $\{d_c\}$; CV metrics for Task A/B

Step 1: Task typing (Sec. 3.1)

- 1: **for** $i = 1$ to N **do**
- 2: $e_i \leftarrow f_{\text{enc}}(p_i)$
- 3: $x_i \leftarrow g(e_i)$
- 4: **end for**
- 5: $\{c_i\}_{i=1}^N \leftarrow \text{KMeans}(\{x_i\}, K)$
- 6: Optionally: assign human-readable labels to clusters via representative keywords

Step 2: Preference-derived signals (Sec. 3.2–3.3)

- 7: **for** each cluster $c \in \{1, \dots, K\}$ **do**
- 8: $\mathcal{D}_c \leftarrow \{(i, y_i) \in \mathcal{R} : c_i = c\}$
- 9: $d_c \leftarrow \frac{1}{|\mathcal{D}_c|} \sum_{(i, y_i) \in \mathcal{D}_c} \mathbb{I}[y_i = \text{tie}]$ ▷ Eq. 5
- 10: **end for**
- 11: **for** each model/agent m and cluster c **do**
- 12: $\mathcal{D}_{m,c} \leftarrow \{(i, y_i) \in \mathcal{R} : c_i = c \wedge (m = m_A \vee m = m_B)\}$
- 13: $w_{m,c} \leftarrow \frac{1}{|\mathcal{D}_{m,c}|} \sum_{(i, y_i) \in \mathcal{D}_{m,c}} \mathbb{I}[y_i = m]$ ▷ Eq. 4
- 14: **end for**

Step 3: Validation probes (Sec. 4)

- 15: Partition data into stratified F folds by outcome label for cross-validation
 - 16: **for** $f = 1$ to F **do**
 - 17: $\mathcal{R}_{\text{train}}, \mathcal{R}_{\text{test}} \leftarrow \text{Split}(\mathcal{R}, f)$
 - Task A (winner prediction).**
 - 18: Construct features $\phi_A(i)$ for each record in $\mathcal{R}_{\text{train}}$: one-hot model IDs (m_A, m_B) + one-hot cluster c_i + response-embedding diff $(e_A - e_B)$
 - 19: Train multinomial logistic regression (optionally with regularization) on $\mathcal{R}_{\text{train}}$
 - 20: Evaluate on $\mathcal{R}_{\text{test}}$ and record accuracy
 - Task B (difficulty prediction).**
 - 21: Construct features $\phi_B(i)$ for each record in $\mathcal{R}_{\text{train}}$: one-hot cluster c_i + winner-combination indicators + prompt length
 - 22: Train ridge regression (optionally compare with none/lasso) on $\mathcal{R}_{\text{train}}$
 - 23: Evaluate on $\mathcal{R}_{\text{test}}$ and record MSE
 - 24: **end for**
 - 25: Report mean CV metrics across folds; optionally run cluster-feature ablation by removing one-hot c_i and re-evaluating
-

B Additional Visualizations

Algorithm 3 Task typing and preference signal computation**Require:** Prompts \mathcal{P} , comparisons \mathcal{D} , encoder f_{enc} , reducer $g(\cdot)$, K , threshold δ **Ensure:** Task types $\{c_i\}$, capability $w_{m,c}$, risk cue d_c

```

1: for  $p_i \in \mathcal{P}$  do
2:    $e_i \leftarrow f_{\text{enc}}(p_i)$ ;  $x_i \leftarrow g(e_i)$ 
3: end for
4:  $\{C_j\}_{j=1}^K \leftarrow \text{Cluster\_Method}(K - \text{Means})(\{x_i\}, K)$ 
5: Reassign small clusters ( $|C_j| < \delta$ ) to nearest large cluster by centroid distance
6: for  $(p_i, m_A, m_B, y_i) \in \mathcal{D}$  do
7:    $c_i \leftarrow \text{cluster}(p_i)$  ▷ prompt  $\rightarrow$  task type
8:   Align vote outcome to  $(m_A, c_i)$  and  $(m_B, c_i)$ 
9: end for
10: Compute  $w_{m,c}$  and  $d_c$  by aggregated counts over aligned comparisons

```

Task	5-fold CV (Regularization)			5-fold CV (Ablation; Ridge)		
	None	Ridge	Lasso	With cluster	Without cluster	Δ
A (Acc \uparrow)	0.543	0.548	0.545	0.548	0.541	+0.007
B (MSE \downarrow)	2.465	2.463	3.664	2.463	2.567	-0.104

Table 1. **5-fold cross-validation results.** Left: regularization sweep for Task A (winner prediction) and Task B (difficulty prediction). Right: effect of task-typing (cluster) features under Ridge (best-performing regularizer).

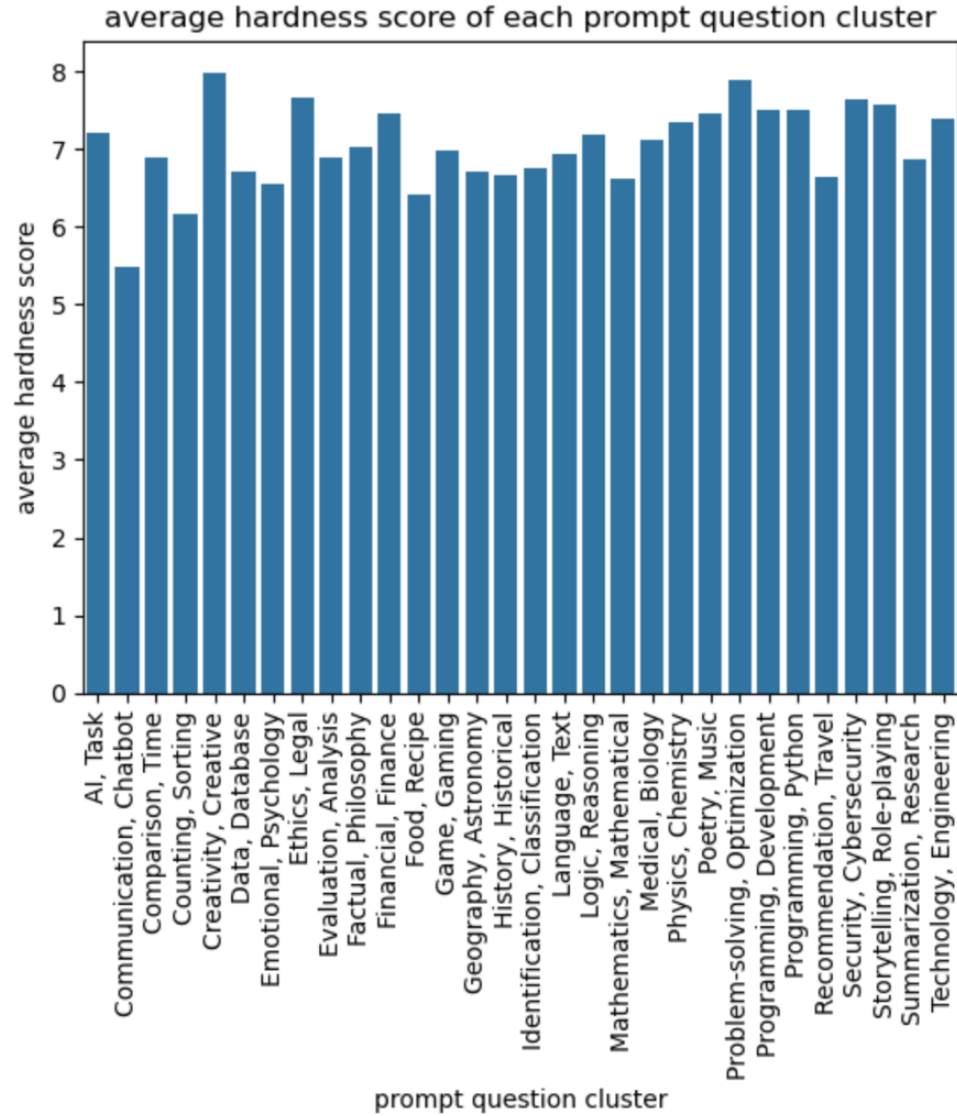


Fig. 2. **Uncertainty / Coordination Risk by Task Type.** We report a task-type-level proxy for uncertainty (e.g., tie rate / disagreement-derived hardness) aggregated within each cluster. Higher values indicate stronger model disagreement and thus elevated coordination risk, motivating safeguards such as clarification and auditing (Sec. ??).

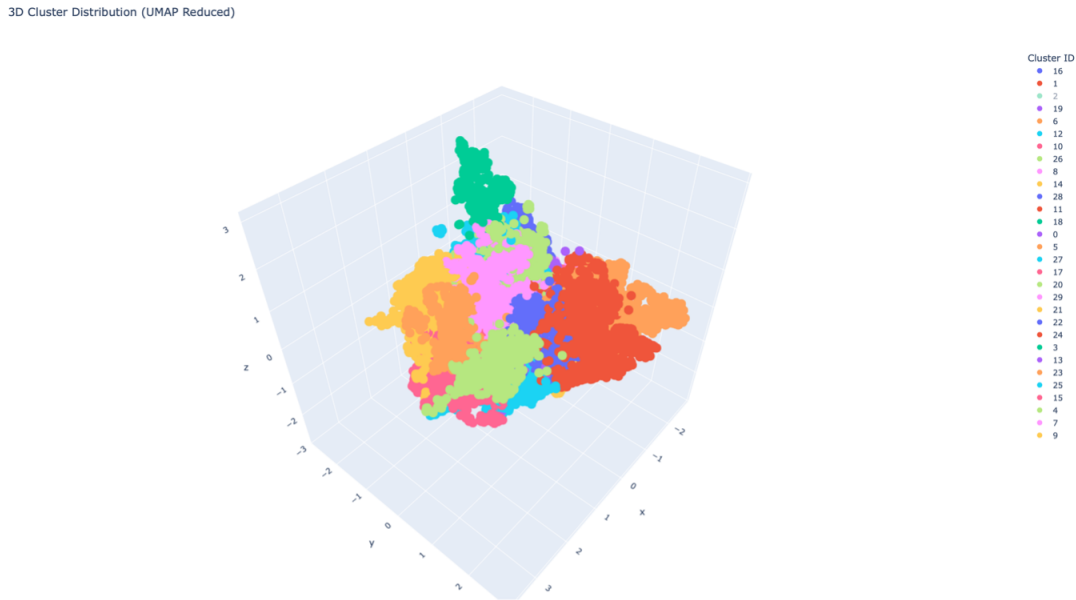


Fig. 3. **Task space visualization.** Low-dimensional projection of prompt embeddings, colored by cluster assignment ($K = 30$), illustrating the induced task-typing structure used throughout Sec. 3.1.

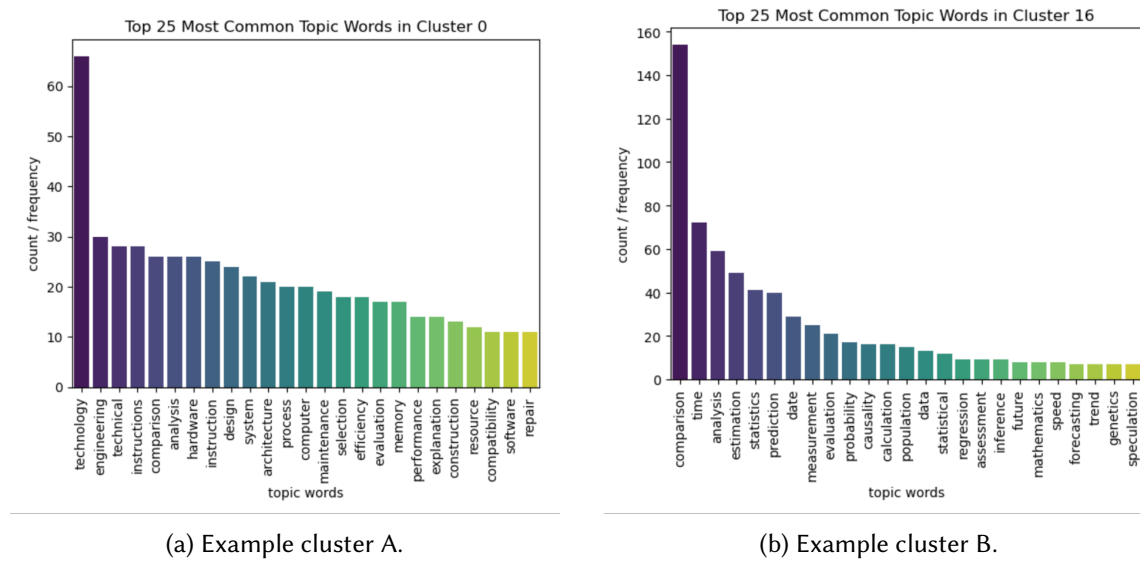


Fig. 4. **Interpretable task labels via cluster keywords.** Representative topic words for two clusters, used to assign human-readable labels and to support common-ground negotiation in task typing (Sec. 3.1).

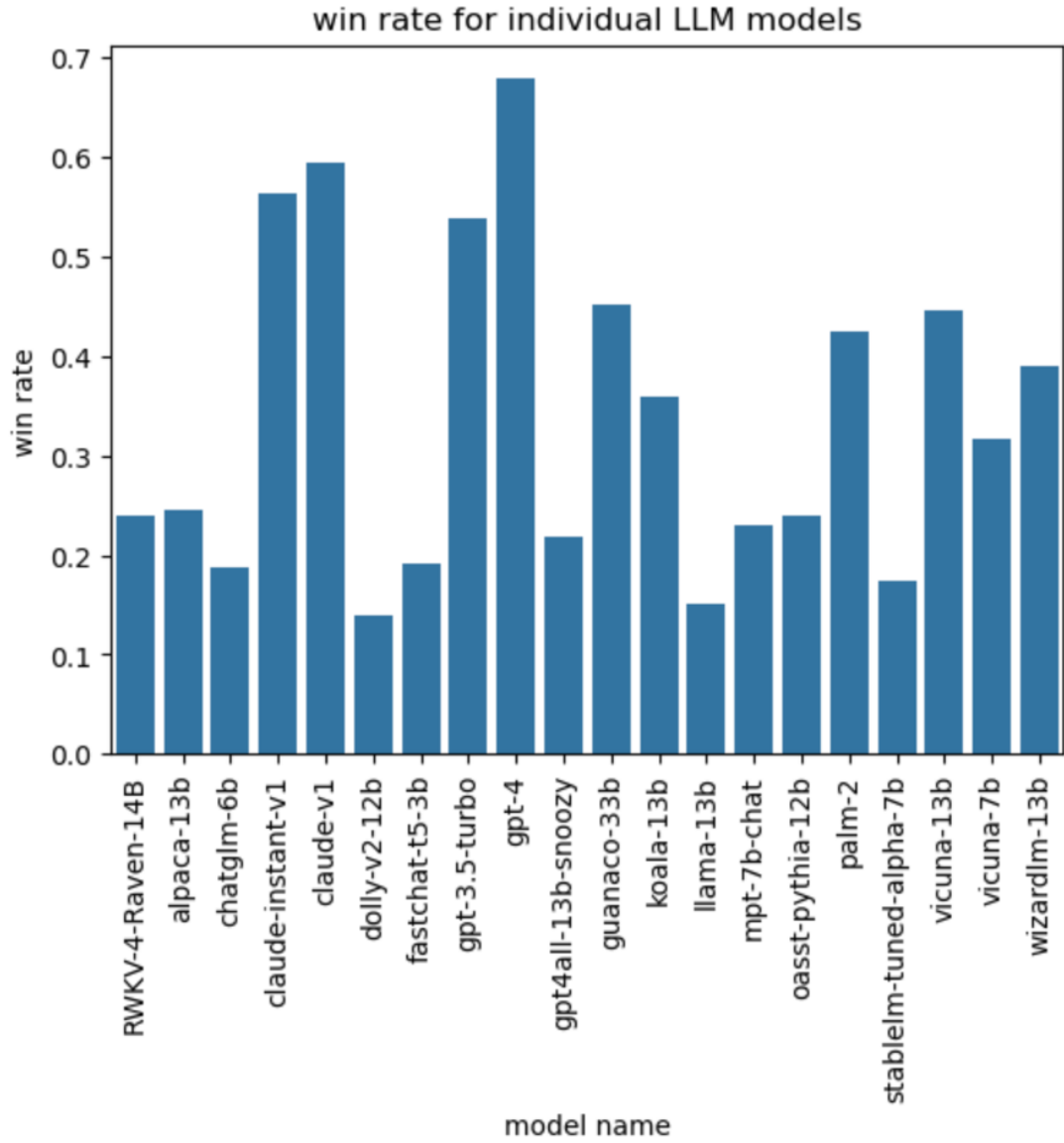


Fig. 5. **Overall preference win rate across tasks.** Aggregate win rates across all prompts. We treat this as a global baseline; our focus is the task-conditioned profiles in Fig. 6.

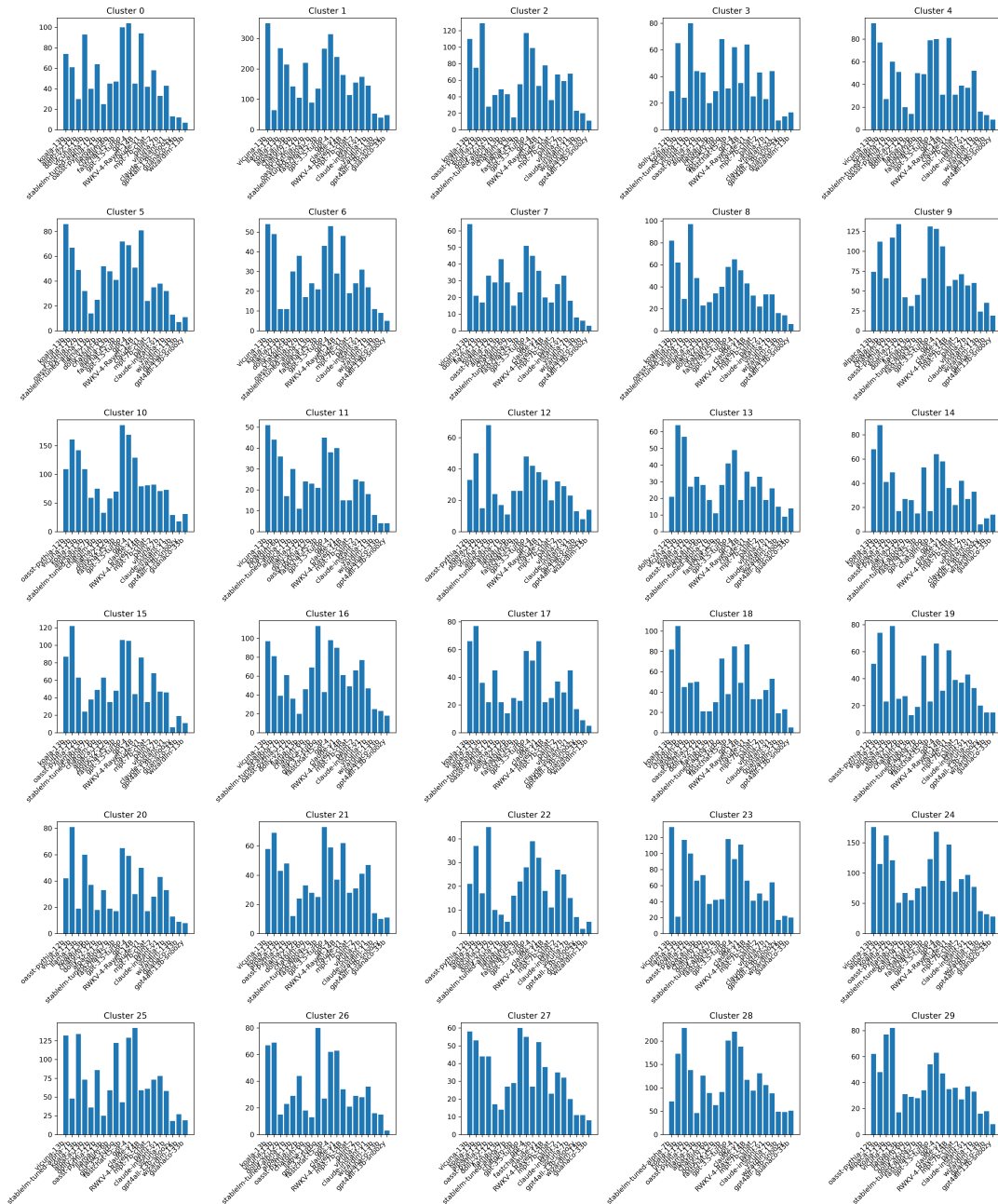


Fig. 6. **Capability Profile Map (task-conditioned preference)**. Each task cluster induces a distinct winner distribution across candidate agents, yielding a task-conditioned capability profile. *Delegation rule:* for cluster c , select the top-1 agent as the primary collaborator; when coordination risk is high (Sec. 3.3), assign an auditor agent.